Early Warning Potential of Low-Cost Sensors Evaluated Using the Camp Mystic Flash-Flooding Event

Ayman Mokhtar Nemnem, S.M.ASCE[1], Md Asifuzzaman Khan[2], Austin R.J. Downey[3] and Jasim Imran, F.ASCE[4]

[1]Dept. of Civil and Environmental Engineering, University of South Carolina, 300 Main St., Columbia, SC 29208. ORCID: https://orcid.org/0009-0003-0238-4394; Email: amokhtar@email.sc.edu
[2]Dept. of Mechanical Engineering, University of South Carolina, 300 Main St., Columbia, SC 29208; ORCID: https://orcid.org/0000-0002-2612-8913; Email: asifuzzaman@sc.edu
[3]Dept. of Mechanical Engineering and Dept. of Civil and Environmental Engineering, University of South Carolina, 300 Main St., Columbia, SC 29208; ORCID: https://orcid.org/0000-0002-5524-2416; Email: austindowney@sc.edu
[4]Dept. of Civil and Environmental Engineering, University of South Carolina, 300 Main St., Columbia, SC 29208. (Corresponding author). ORCID: https://orcid.org/0000-0002-3479-3905; Email: imran@sc.edu

ABSTRACT

Extreme rainfall can trigger rapid flash flooding in small watersheds, often leaving limited time to respond. In ungauged basins, the lack of upstream rainfall or stage measurements further constrains the ability to track evolving conditions. This study reconstructs the July 4th, 2025, Camp Mystic flood in Kerr County, Texas, and examines the feasibility of upstream early warning using low-cost water-level sensors. A two-dimensional HEC-RAS model was developed using 10-m USGS terrain data, land-cover-based Manning's n from NLCD, and rainfall observations from nearby stations. The simulation reproduced an approximately 11-m rise in water level within five hours and showed satisfactory agreement with documented high-water marks. Potential upstream sensing locations were identified using the Topographic Wetness Index (TWI). Stage hydrographs extracted at these points show a much faster and earlier rise than at the downstream site, providing a meaningful lead time for evacuation. Comparisons with 100-yr and 1000-yr SCS Type II storms show that the observed stage rose much more rapidly than standard design storms. The results indicate that low-cost, off-grid sensors, when deployed using combined hydrodynamic and terrain-index analysis, can support practical early-warning capability in steep, ungauged headwater basins.

INTRODUCTION

Flash floods in small watersheds can develop rapidly during high-intensity rainfall, often providing little advance warning. In ungauged basins, the absence of upstream rainfall and streamflow measurements limits the ability to track changing hydrologic conditions. Headwater catchments with steep slopes, limited soil storage, and closely spaced tributaries are especially prone to fast runoff generation and abrupt rises in stage (Özgen-Xian et al., 2023). Several recent extreme-rainfall events have shown how quickly floods can develop in such environments. In the United States, the July 4th, 2025 floods in Kerr County, Texas, and Hurricane Helene's 2024 flooding in Asheville, North Carolina, produced rapid increases in flow that exceeded local response capacity (Amorim et al., 2025). Internationally, intense rainfall in 2023 led to the failures of the Derna dams in Libya, resulting in cascading breaches and substantial loss of life (Nemnem et al., 2025). These cases reflect the challenges of anticipating conditions in ungauged basins where upstream data are unavailable.

Flash-flood forecasting in the United States relies on ground-based rain gauges, NEXRAD radar, satellite precipitation estimates, and USGS stream gages. These observations support hydrologic and hydrodynamic forecasting systems such as the National Water Model (NWM), while numerical weather prediction models (e.g., HRRR, GFS, GEFS) provide atmospheric forcing (National Weather Service, NOAA, 2025b; Office of Water Prediction, NOAA, 2025). Other tools, including FLASH and the Flash Flood Guidance System (FFGS), estimate near-term flood potential using rainfall intensity thresholds and basin susceptibility (National Weather Service, NOAA, 2025a). Despite these capabilities, many headwater watersheds remain ungauged, leaving downstream communities with limited advance notice even when regional forecasts indicate elevated risk. This condition was a factor in the July 4th, 2025 Kerr County flooding, which caused more than 130 fatalities region-wide, including 27 at Camp Mystic (ABC News, 2025; CBS, 2025; Houston Chronicle, 2025; NBC News, 2025).

Low-cost, off-grid, IoT-enabled water-level sensors have become feasible for remote monitoring. These devices pair low-power electronics with long-range wireless communication and can operate for extended periods using primary cells or small solar panels. Communication options such as LoRa, NB-IoT, or Wi-Fi can be selected based on local constraints. Commercial devices illustrate current capabilities. For example, the HOBOnet Water Level Sensor Interface complete set (approximately USD 900) uses an off-grid power design, reports a wireless range of roughly 2,000 ft, and specifies a multiyear operating life (HOBO, 2025). Proprietary systems, however, typically do not provide access to hardware or firmware, which limits customization and repair.

Open designs address these constraints by providing bills of materials, firmware, and design files. For instance, an openly documented ultrasonic water-level sensor developed at the University of South Carolina uses a compact enclosure, operates on low power, and transmits data over roughly 100 m (ARTS Lab, n.d.; Smith et al., 2022). A rechargeable Li-Po battery with solar assistance supports about two weeks of unattended operation, and magnetic mounts allow rapid attachment to structures such as bridge rails. The bill of materials is approximately USD 200, and the small form factor enables straightforward field installation and replacement.

Determining whether such sensors could have provided a useful lead time during the July 4th event requires a reconstruction of the flood. Forensic hydrodynamic modeling resolves flood routing, timing, velocity fields, and inundation patterns, which are needed to evaluate upstream warning potential. Terrain indicators such as the Topographic Wetness Index (TWI) can identify runoff-convergence zones that may serve as effective sensor locations.

This study reconstructs the July 4th Camp Mystic flood and evaluates the potential for upstream monitoring to provide additional early-warning lead time in an ungauged headwater system. A two-dimensional hydrodynamic model was developed using the Hydrologic Engineering Center's River Analysis System (HEC-RAS) software to simulate flood propagation across the watershed. Terrain analysis using the TWI was used to locate probable convergence zones and candidate upstream sensing points. The results show that low-cost, off-grid sensors, when guided by hydrodynamic modeling and terrain-based metrics, can be used to augment flash-flood monitoring capability in ungauged basins.

STUDY AREA

The study area is the 225 km² South Fork Guadalupe River headwater basin in Kerr County, Texas—an ungauged tributary of the Guadalupe River. The watershed contains steep to moderately rolling terrain that facilitates rapid runoff generation during high-intensity rainfall. Land cover is dominated by evergreen forest and shrub/scrub vegetation. The basin extends roughly 30 km west–east and contains nearly 700 m of elevation relief, contributing to short hydrologic response times during extreme storms.

Camp Mystic, the primary downstream point of interest, is located on the floodplain near the confluence of the South Fork Guadalupe, Cypress Creek, and a smaller intermittent tributary locally referred to as Bubble Gum (Goodman et al., 2025). Dormitories, gathering areas, and recreational facilities are positioned close to the active channel, leaving little natural buffer between the river and occupied structures. This arrangement increases the site's exposure to abrupt stage changes during flash-flood conditions. The watershed has no upstream rainfall or streamflow monitoring stations and no automated warning systems. As a result, awareness of evolving hydrologic conditions depends largely on regional forecasts and downstream observations.

During the July 4th, 2025 flash flood, approximately 250–304 mm (10–12 in) of rain fell over roughly six hours, corresponding to a 1-in-1000-year rainfall intensity classification (NOAA Physical Sciences Laboratory, 2025). Figure 1 shows the watershed boundary, major tributary network, and the location of Camp Mystic.

METHODOLOGY

A two-dimensional hydrodynamic model of the South Fork Guadalupe River watershed was developed in HEC-RAS to simulate flood-wave propagation and floodplain hydraulics during the July 4th event. The model solves the depth-averaged shallow-water equations using the Eulerian–Lagrangian Method (SWE-ELM), which is appropriate for representing rapidly varying flows and high velocities typical of flash-flood conditions.

A variable-resolution computational mesh was used: 10-m cells were assigned along main channels, tributaries, and throughout the Camp Mystic property to resolve velocity gradients, confluence interactions, and building obstruction effects, while 20–30 m cells were applied to upland and wider floodplain areas to reduce computational cost without compromising the representation of primary flow pathways. The final computational domain contained approximately 700,000 cells. Excess precipitation was applied as a spatially uniform distributed load over the grid, and a normal-depth boundary condition was specified at the watershed outlet.

A 10-m United States Geological Survey (USGS) 3DEP digital elevation model (DEM) served as the primary terrain dataset (United States Geological Survey, 2021). The DEM was hydrologically conditioned to remove sinks and maintain drainage continuity. Spatially varying surface roughness was assigned using the National Land Cover Database (NLCD 2021) (United States Geological Survey, 2025), with each land-cover class mapped to a Manning's n value representing vegetation, developed surfaces, and riparian areas. Figure 1 illustrates the USGS 10-m DEM and NLCD land-cover map of the South Fork Guadalupe watershed.

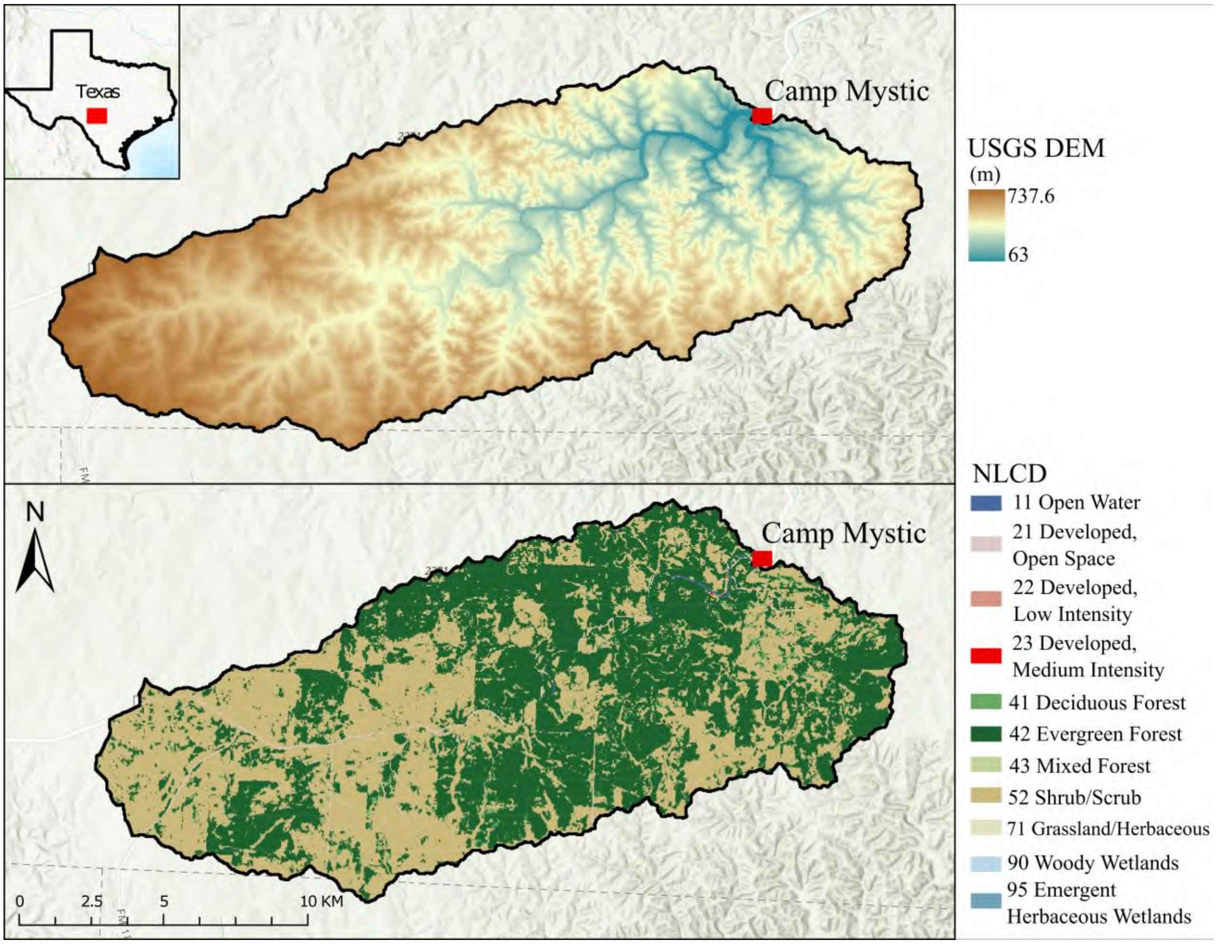

Figure 1. USGS 10-m DEM (top) and NLCD 2021 land-cover map (bottom) of the South Fork Guadalupe watershed, including the location of Camp Mystic.

Rainfall losses were estimated using a mean Curve Number (CN) of 87.6, representing aggregated watershed land cover and soil characteristics, utilizing the Global Curve Number (GCN250) dataset (Jaafar et al., 2019). The CN value was used to compute initial abstraction and infiltration losses in generating the excess rainfall hyetograph. Rainfall time series were obtained from USGS station 08165500 (Guadalupe River at Hunt, TX), which recorded the hourly evolution of the July 1–8 storm system responsible for the July 4th flash flood.

Reports from the NOAA Physical Sciences Laboratory indicate that 250–304 mm (10–12 in) of rainfall fell across the region during the event (NOAA Physical Sciences Laboratory, 2025). Because the Southfork Guadalupe watershed is ungauged and the NOAA estimate reflects the upper bound of observed totals, a total rainfall depth of 304 mm (12 in) was applied in the model. The resulting excess rainfall hyetograph was applied uniformly across the watershed, consistent with the spatial uniformity of rainfall reported during the event. Figure 2 presents the cumulative rainfall, losses, and excess rainfall used as hydrodynamic input.

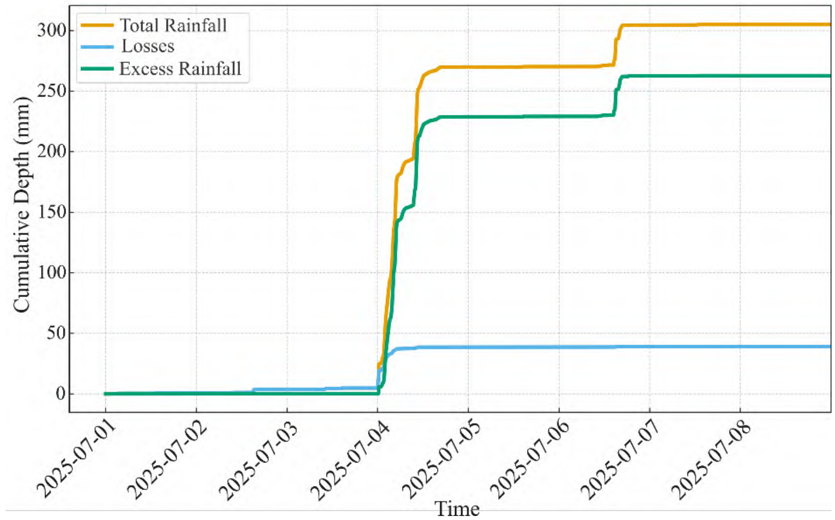

Figure 2. Cumulative total rainfall, losses, and excess rainfall for the July 1- 8, 2025 event.

Identification of Potential Sensor Placement Locations. Terrain-based indicators were used to support the identification of possible upstream locations suitable for early-warning instrumentation. The Topographic Wetness Index (TWI) is a terrain-based metric that identifies areas where runoff is likely to accumulate and initiate surface flow (Sørensen et al., 2006). It is defined as:

$$TWI = \ln\left(\frac{a}{\tan\beta}\right), \tag{1}$$

Where a = upslope contributing area per unit contour width, representing the amount of land draining to a point, and β= local slope angle (in radians). The larger of (a) values indicate greater potential for runoff concentration, while the lower slopes (small β) promote water pooling and early saturation. Figure 3 shows the TWI map and candidate locations for sensor placement. Areas with high TWI values represent preferential flow pathways where rising water levels can be detected before downstream flooding occurs.

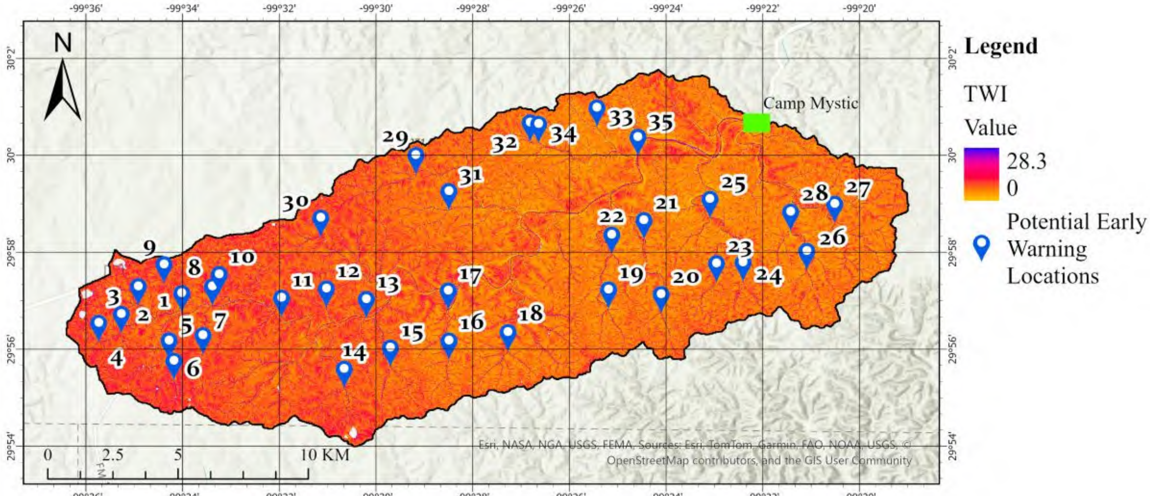

Figure 3. Topographic Wetness Index (TWI) map of the watershed with proposed upstream sensor locations based on runoff-convergence zones.

RESULTS AND DISCUSSIONS

The two-dimensional hydrodynamic simulations reproduced the rapid rise in water surface elevation associated with the July 4th flash-flood event. Water levels increased sharply throughout the lower tributary network due to limited channel storage, steep slopes, and short flow travel distances. At the confluence near Camp Mystic, simulated stages rose by approximately 11 m within five hours, consistent with the extremely short hydrologic response expected in a high-gradient headwater basin. Peak discharge exceeded 1,700 m³/s, generating extensive floodplain inundation, high lateral velocities, and localized zones of elevated shear stress around buildings and other structural obstructions. Figures 4a–c summarize the hydraulic response: watershed-scale inundation depth and extent, the simulated flow hydrograph at the Camp Mystic location, and maximum inundation patterns within the camp, including flow streamlines and digitized building footprints. Table 1 compares simulated peak water levels with observed high-water marks reported near several Camp Mystic cabins (Goodman et al., 2025), showing close agreement between modeled and observed stages.

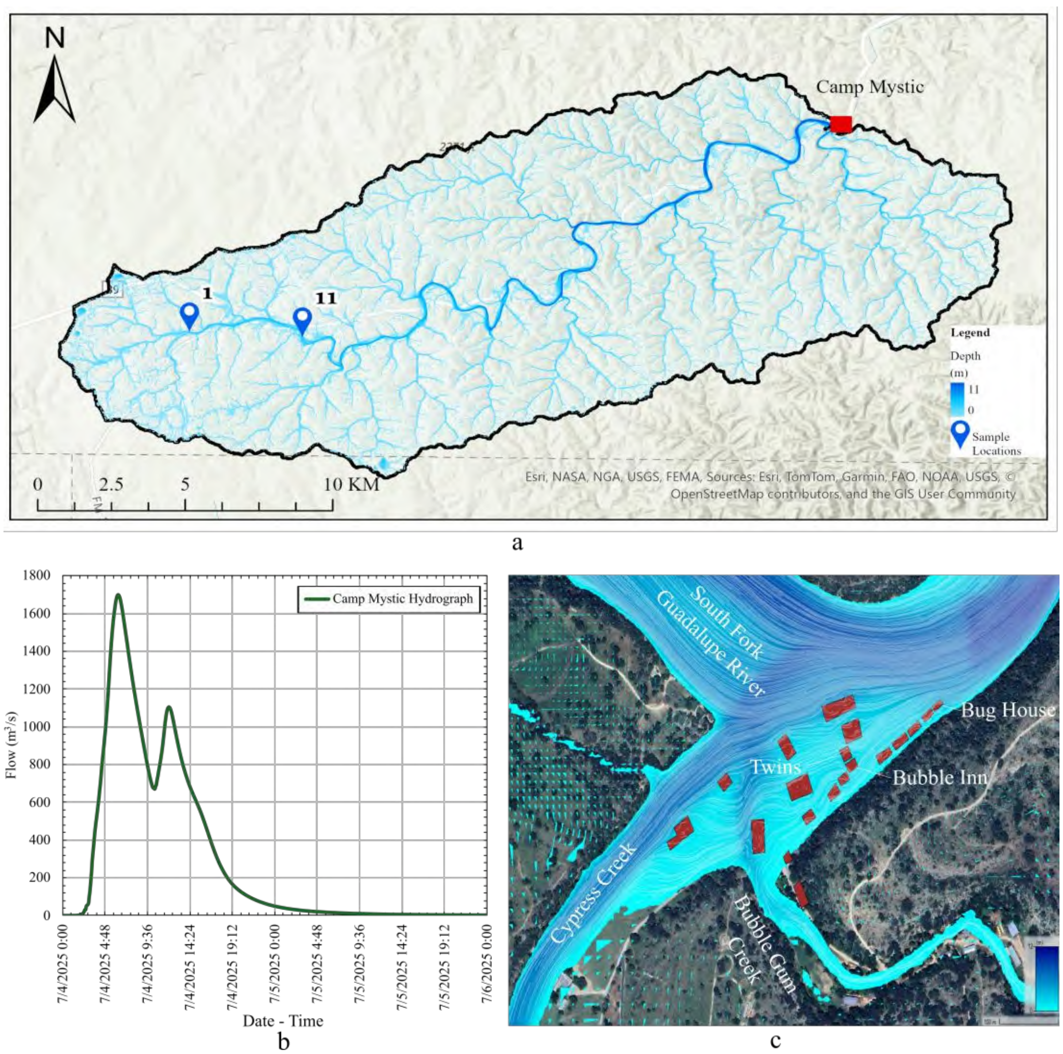

Figure 4. (a) Watershed-scale flood inundation depth and extent simulated for the July 4th, 2025 event. (b) Flow hydrograph at the Camp Mystic location extracted from the 2D hydrodynamic model. (c) Maximum flood inundation depth and extent in the vicinity of Camp Mystic, including flow streamlines and digitized building footprints.

Table 1: Observed and simulated peak water levels for the July 4th flood at Camp Mystic Cabins.

Location	Observed (m)	Simulated (m)
Bubble Inn Cabins	1.9	1.7
Twins Cabins	2.2	2.0
Bug House Cabins	2.7	2.8

The upstream reference points, identified using the Topographic Wetness Index, indicate clear opportunities for early detection of the advancing flood wave. After comparing simulated stage hydrographs at all candidate locations shown in Figure 3, Points 1 and 11 were selected as the stage hydrograph at these locations exhibited the earliest and most pronounced response with clear lead-time advantages. As shown in Figure 5a, the stage rise at both upstream locations begins well before noticeable increases occur downstream. Table 2 summarizes the spatial variability in rising rates, which offers additional insight into the flood's rapid evolution and the value of upstream sensing. During the first two hours of runoff concentration, both upstream points exhibited substantial and accelerating rise rates compared with Camp Mystic. In the first hour, Reference Point 1—the most upstream location—showed a rise rate of 634 mm/hr, while the downstream, Camp Mystic, increase was only 230 mm/hr. A similar pattern emerged in the second hour, with Reference Point 11 rising at 1,212 mm/hr, compared with 657 mm/hr at Camp Mystic. These differences indicate that the tributaries began rising sharply well before hazardous conditions developed downstream. Although Camp Mystic initially experienced modest increases, the downstream rise accelerated markedly during the third and fourth hours, reaching 2,317 mm/hr and 3,711 mm/hr, respectively, as floodwaters converged into the main channel. This progression demonstrates that upstream sensing locations provide the earliest and most informative indicators of the approaching flood wave, which establishes their importance for effective early-warning deployment in ungauged headwater basins.

Table 2: Hourly stage-rise rates (mm/hr) at two upstream reference points and at Camp Mystic.

Time Since Onset	Reference Point 1 (mm/hr)	Reference Point 11 (mm/hr)	Camp Mystic (mm/hr)
1st hour	634	267	230
2nd hour	864	1,212	657
3rd hour	1,773	1,706	2,317
4th hour	–142*	1,601	3,711

*Negative value indicates stage drawdown after peak stage.

Comparison with Synthetic Design Storms. To provide context for the extremely fast-rising rates observed during the July 4th event, two additional simulations were performed using synthetic SCS Type II design storms. The 100-year and 1000-year events, with corresponding 24-hour rainfall depths of 284 mm and 466 mm, were applied across the watershed to evaluate how conventional design storms compare to the real event's hydrologic extreme. As shown in Figure 5b, the stage hydrographs demonstrate the exceptional severity of the July 4th event. The actual event reached a peak stage of 10.6 m in only 6.3 hours, corresponding to an effective stage rise rate of approximately 1,676 mm/hr. In contrast, the 100-year SCS Type II storm produced a slower rise to 12.3 m in 13.4 hours (~ 918 mm/hr), while the 1000-year storm generated 15.3 m in 13.1 hours (~ 1,168 mm/hr). Although the synthetic storms yield a higher peak, their rise is substantially more gradual than the real event. This comparison indicates that the July 4th flood evolved substantially faster than even the most extreme synthetic design storms, which emphasize the importance of upstream real-time sensing and localized early-warning strategies in steep, ungauged basins.

Table 3 summarizes the hourly stage-rise rates for the 1000-yr SCS Type II synthetic storm and shows a pattern consistent with that observed during the July 4th event. During the initial hours of runoff concentration, the upstream locations again exhibited earlier and more pronounced stage-rise behavior compared with Camp Mystic. In the first hour, Reference Point 1 showed a rise rate of 350 mm/hr, while the downstream rise at Camp Mystic was only 150 mm/hr. A similar pattern appears in the second hour, with Reference Point 11 rising at 540 mm/hr, compared with 150 mm/hr at the downstream location. These similarities indicate that the same upstream tributary points respond earliest not only under observed extreme rainfall, but also under synthetic design storm forcing. This reinforces that these locations could be identified in advance, before an actual flood, using hydrodynamic and terrain-based analysis to guide sensor placement for early-warning applications.

Table 3: Hourly stage-rise rates (mm/hr) at two upstream reference points and at the Camp Mystic location for the 1000-year SCS Type II synthetic storm simulation.

Time Since Onset	Reference Point 1 (mm/hr)	Reference Point 11 (mm/hr)	Camp Mystic (mm/hr)
1st hour	350	0	150
2nd hour	500	540	150
3rd hour	370	700	640
4th hour	170	460	580

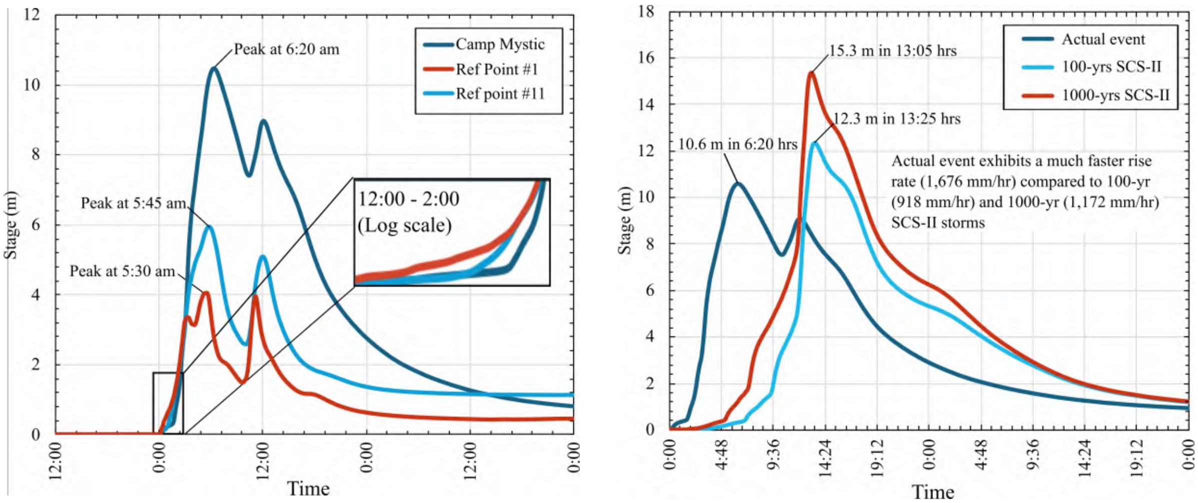

a b

Figure 5. (a) Simulated stage hydrographs at Camp Mystic and two upstream reference points. (b) Comparison of the July 4th, 2025 event with 100-yr and 1000-yr SCS Type II storms.

Upstream Monitoring and Early-Warning Potential. Off-grid power and long-range wireless communication enable the deployment of low-cost water-level sensors in headwater locations where conventional hydrometric stations are absent. Modular housings and swappable components allow rapid installation and recovery, while each sensor transmits measurements wirelessly to a base station that provides storage and cellular backhaul. Figure 6 demonstrates a recent installation of water height sensors in the City of Hanahan, Charleston, to monitor water height at the confluence of Goose and Turkey Creek and a small tributary of Turkey Creek. Clustering several sensors along tributaries creates a distributed stream of stage observations that can capture rising water as it propagates downstream. Spatial cross-checks between adjacent nodes help filter outliers and reduce false alarms, and short sampling intervals support near–real-time tracking. Even with intermittent connectivity, base stations can buffer data and forward measurements when communication resumes. Taken together, the outcome is a community-maintained network of low-cost sensors that could feasibly deliver timely flood warnings in remote or poorly instrumented watersheds such as Camp Mystic.

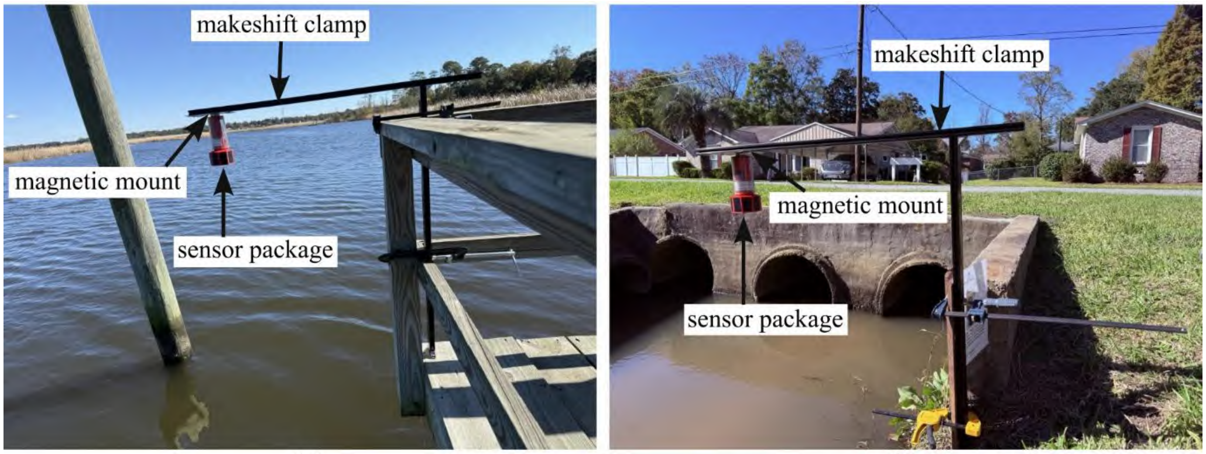

(a) (b)

Figure 6. Two SWaP-constrained packages deployed in the City of Hanahan, Charleston, SC

CONCLUSION

This study reconstructed the hydrodynamics of the July 4th, 2025 flash flood at Camp Mystic and evaluated the feasibility of early warning using low-cost water-level sensors in an ungauged headwater watershed. The hydrodynamic model captured the rapid water-level rise, approximately 11 m within five hours, and showed that upstream tributaries reacted several hours before conditions intensified at the camp. At one upstream location, the stage rose to 1 m nearly five hours before the peak at Camp Mystic, indicating that targeted sensor placement could provide meaningful advance notice. Combining terrain-based metrics such as the Topographic Wetness Index (TWI) with hydrodynamic model results provides a systematic method for identifying promising sensor locations. A comparison with synthetic 100-year and 1000-year SCS Type II storms showed that the July 4th event produced a much sharper rise and earlier peak than standard design storms.

The results demonstrate that low-cost, field-deployable sensors offer a practical way to improve flash-flood readiness in ungauged basins. When paired with hydrodynamic modeling and terrain analysis, these networks can deliver useful lead time and improve the ability of downstream communities to respond during rapidly developing headwater floods. Future work should include field deployment and testing of sensor arrays, refinement of automated thresholding methods, and coordination with local emergency procedures.

ACKNOWLEDGEMENTS

The authors gratefully acknowledge support from the National Science Foundation (Award 2152896), the Office of Naval Research (Grant N000142412727), the U.S. Army Corps of Engineers Engineer Research and Development Center (Award W912HZ-21C-0067), and the National Oceanic and Atmospheric Administration through the Cooperative Institute for Research to Operations in Hydrology (CIROH, NA22NWS4320003).

REFERENCES

ABC News. (2025, July 29). *Texas floods: 911 audio from county near hard-hit Kerrville shows confusion and distress*. https://abcnews.go.com/US/texas-floods-911-audio-county-hard-hit-kerrville/story?id=124184244

Amorim, R., Villarini, G., Czajkowski, J., & Smith, J. (2025). Flooding from Hurricane Helene and associated impacts: A historical perspective. *Journal of Hydrology X*, *27*, 100204. https://doi.org/10.1016/j.hydroa.2025.100204

ARTS-Lab. (n.d.). *UAV Deployable Stage Height Sensor*. https://github.com/ARTS-Laboratory/UAV-Deployable-Stage-Height-Sensor

CBS. (2025, August 8). *Officials release names of July 4 flood victims in Kerr County*. https://www.cbsnews.com/texas/news/central-texas-flood-victims-kerr-county-dallas-fort-worth/

Goodman, J. D., Khurana, M., Erden, B., Hernandez, M., Liu, Y., Patanjali, K., Saget, B., & Smart, C. (2025, November 15). *Swept Away: A detailed account of how 28 people died in the flooding at Camp Mystic*. The New York Times; The New York Times. https://www.nytimes.com/interactive/2025/11/15/us/camp-mystic-flooding-deaths-video-map.html

HOBO, O. (2025). *HOBOnet Water Level Sensor*. https://www.onsetcomp.com/products/sensors/rxw-wl?v=RXW-WL-868

Houston Chronicle. (2025, July 7). *Texas flooding: Death toll in Kerr County rises to 84, as Camp Mystic confirms loss of 27 campers*. https://www.houstonchronicle.com/news/houston-texas/texas/article/texas-flood-latest-20758660.php

Jaafar, H. H., Ahmad, F. A., & El Beyrouthy, N. (2019). GCN250, new global gridded curve numbers for hydrologic modeling and design. *Scientific Data*, *6*(1), 145. https://doi.org/10.1038/s41597-019-0155-x

National Weather Service, NOAA. (2025a). *Flash Flood Guidance System (FFGS)*. https://www.weather.gov/nerfc/FFG

National Weather Service, NOAA. (2025b). *Forecast Models Overview: GFS, GEFS, HRRR*. https://www.weather.gov/mdl/gfsguide

NBC News. (2025, July). *Texas flooding unfolded as deadly Kerr County, Camp Mystic flash-flood disaster*. https://www.nbcnews.com/news/us-news/texas-flooding-unfolded-deadly-kerrville-camp-mystic-rcna217712

Nemnem, A. M., Tanim, A. H., Nahian, A., Khan, S., Goharian, E., & Imran, J. (2025). How extreme rainfall and failing dams unleashed the Derna flood disaster. *Nature Communications*, *16*(1), 4191. https://doi.org/10.1038/s41467-025-59261-9

NOAA Physical Sciences Laboratory. (2025, August 11). *Weather Whiplash in Texas: Drought to Flood in Central Texas*. https://psl.noaa.gov/news/2025/texasfloods.html#:~:text=Starting%20on%20July%203%2C%20remnant,six%20hours%20over%20some%20locations.

Office of Water Prediction, NOAA. (2025). *National Water Model Overview*. https://water.noaa.gov/about/nwm

Özgen-Xian, I., Molins, S., Johnson, R. M., Xu, Z., Dwivedi, D., Loritz, R., Mital, U., Ulrich, C., Yan, Q., & Steefel, C. I. (2023). Understanding the hydrological response of a headwater-dominated catchment by analysis of distributed surface–subsurface interactions. *Scientific Reports*, *13*(1), 4669. https://doi.org/10.1038/s41598-023-31925-w

Smith, C., Satme, J., Martin, J., Downey, A. R. J., Vitzilaios, N., & Imran, J. (2022). UAV rapidly-deployable stage sensor with electro-permanent magnet docking mechanism for flood monitoring in undersampled watersheds. *HardwareX*, *12*, e00325. https://doi.org/10.1016/j.ohx.2022.e00325

Sørensen, R., Zinko, U., & Seibert, J. (2006). On the calculation of the topographic wetness index: Evaluation of different methods based on field observations. *Hydrology and Earth System Sciences*, *10*(1), 101–112. https://doi.org/10.5194/hess-10-101-2006

United States Geological Survey. (2021). *United States Geological Survey 3D Elevation Program 1/3 arc-second Digital Elevation Model*.

United States Geological Survey. (2025). *Annual National Land Cover Database (NLCD) Collection 1 Products (ver. 1.1, June 2025)*. U.S. Geological Survey. https://doi.org/10.5066/P94UXNTS